CHAPTER 8

About the Numerical Solution of the Equations of Piezoelectricity

Martin Kögl[1] and Lothar Gaul[2]

[1] Departamento de Engenharia de Estruturas e Fundações, Escola Politécnica, Universidade de São Paulo, Brazil
[2] Institute A of Mechanics, University of Stuttgart, Germany

Abstract. In this paper, the numerical solution of piezoelectric problems by means of two discretization methods – the Finite Element Method (FEM) and the Boundary Element Method (BEM) – is described. At first, using the equations of elastostatics, the similarities and differences of the methods are explained and some of their advantages and disadvantages are pointed out. After this, the piezoelectric formulations of both methods are introduced. A numerical example serves to demonstrate the excellent agreement of the FEM and BEM results as well as to show the superiority of the BEM in the calculation of elastic stresses and the electric field.

1 Introduction

The increasing importance and use of piezoelectric materials in engineering sciences calls for reliable numerical methods that are capable of accurately modelling and solving problems involving piezoelectrics. Besides the FEM, Boundary Element Methods are a very powerful tool for the numerical solution of field problems of mathematical physics, since they offer some inherent advantages over FEM like the discretization of the boundary only, as well as an improved accuracy in stress calculations. In this article, the formulations of both methods are compared, and some of their advantages and disadvantages are pointed out.

2 Finite Element and Boundary Element Methods

This section gives a brief comparison of the Finite Element and Boundary Element Methods. For a more detailed introduction into FEM, the interested reader is referred to the books of Bathe (1996) and Zienkiewicz and Taylor (1991; 1994). The BEM is described in detail in Brebbia et al. (1984) and Gaul and Fiedler (1996).

2.1 General Features

The most striking difference between FEM and BEM, and one of the important advantages of the latter, concerns the discretization. While in FEM the complete domain has to be discretized, in BEM only the discretization of the boundary is required, as seen in Figure 1. Depending on the

V. Kompiš (ed.), *Selected Topics in Boundary Integral Formulations for Solids and Fluids*

complexity of the actual structure and load case under investigation, this simplified discretization can lead to important time savings in the mesh creation and modification process. Other areas in which the BEM possesses certain advantages are problems involving infinite or semi-infinite domains (e.g. acoustics, soil-structure interaction, etc.), as well as stress concentration problems. This is partly due to the use of fundamental solutions, which are *analytical* free space solutions of the governing differential field equations, and can therefore accurately represent far-fields and stresses.

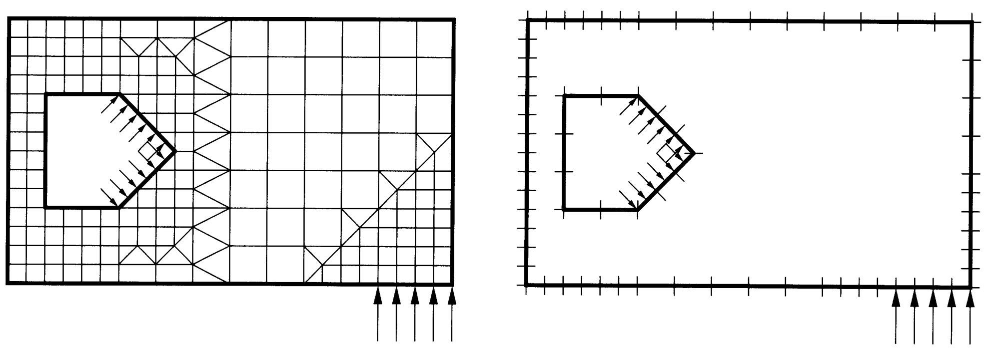

Figure 1. Discretization with finite elements (left) and boundary elements (right)

On the other hand, the fact that a fundamental solution is required poses some problems, e.g., for inhomogeneous and non-linear analyses, where special methods such as the Dual Reciprocity Method (DRM) (Partridge et al., 1992) have to be applied. Since the FEM does not rely on fundamental solutions, it has less difficulties in handling these kinds of problems. Also, in structural mechanics, Finite Element Methods have the advantage of leading to symmetric, positive definite, and sparsely populated matrices, so that special time-saving solvers can be used, whereas the BEM matrices are usually non-symmetric and fully populated.

2.2 Comparison of FE and BE Formulations

This section aims at demonstrating the similarities and differences between the methods by introducing them in a comparative manner, as shown in Figure 2. This is done for the case of linear elastostatics without body forces, in order to concentrate on the essentials. The starting point for both formulations is a weighted residual statement, in which the governing differential equation and boundary conditions are weighted with test functions w. Integration by parts leads to the weak statement, which is the basis of the FEM; further integration by parts results in the inverse statement, which forms the basis of the BEM.

The next steps show some significant differences between the methods. The standard FEM as derived here is a pure displacement formulation, in which only the displacements appear as unknowns. These displacements are approximated by functions which have to fulfill the forced boundary conditions. The stresses and tractions are calculated only after the solution of the displacement field. This involves derivation of the shape functions, which results in a loss of accu-

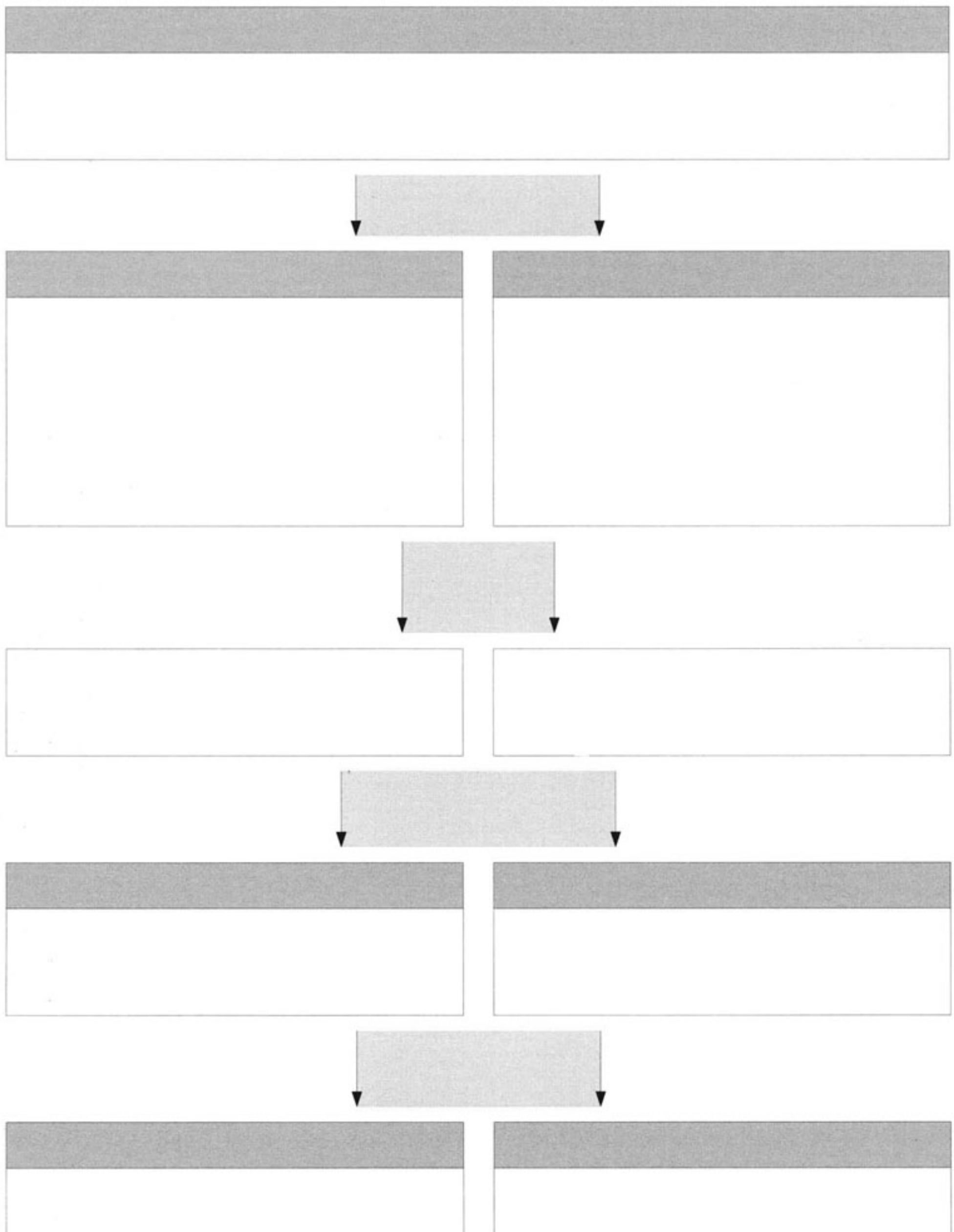

Figure 2. Comparison of Finite Element Method and Boundary Element Method

racy for stress and traction results. On the other hand, the Boundary Element Method is a mixed formulation, containing both displacements and tractions as unknowns. Hence, apart from the displacements, the traction field, too, has to be approximated. The approximation functions now have to fulfill the natural boundary conditions. This is why the results for the tractions obtained with BEM are usually more accurate than those obtained with FEM.

Another difference between the methods lies in the choice of the weighting function. The classical FEM is a Bubnov-Galerkin method, using the same set of functions for the approximation of the displacement field as for the weighting functions. On the other hand, the BEM is a Petrov-Galerkin method, where the weighting functions are chosen as the fundamental solutions of the governing differential equations. This leads to an elimination of the domain integral by virtue of the sifting property of the Dirac impulse, which results in a pure boundary formulation for the unknown displacement and traction fields.

3 Basic Equations of Piezoelectricity

The elastic and electric field of a piezoelectric body are described in terms of elastic displacements u_k and electric potential φ by the differential equations (for more details, see e.g. Kögl (2000) and Tiersten (1969))

$$C_{ijkl}\, u_{k,li} + e_{lij}\, \varphi_{,li} = \rho \ddot{u}_j \; , \tag{1}$$

$$e_{ikl}\, u_{k,li} - \epsilon_{il}\, \varphi_{,li} = 0 \; , \tag{2}$$

with mass density ρ, elasticity tensor C_{ijkl}, piezoelectric tensor e_{lij}, and permittivity tensor ϵ_{il}. Here and in the following, Einstein's summation convention is applied, the comma denotes partial differentiation with respect to the spatial coordinates, and the superimposed dot denotes partial differentiation with respect to time.

The stress tensor σ_{ij} and electric displacement vector D_i are obtained from the constitutive equations

$$\sigma_{ij} = C_{ijkl}\, \varepsilon_{kl} - e_{lij}\, E_l \; , \tag{3}$$

$$D_i = e_{ikl}\, \varepsilon_{kl} + \epsilon_{il}\, E_l \; , \tag{4}$$

where $\varepsilon_{kl} = 1/2(u_{k,l} + u_{l,k})$ denotes the strain tensor and $E_l = -\varphi_{,l}$ denotes the electric field vector. The fluxes are given by

$$t_j = \sigma_{ij}\, n_i \; , \qquad q = D_i\, n_i \; , \tag{5}$$

with traction vector t_j, charge flux density q, and direction vector n_i.

Using a condensed notation, where lower case subscripts range from 1 to 3, and upper case subscripts from 1 to 4, it is possible to combine corresponding elastic and electric quantities into generalized piezoelectric vectors and tensors, which simplifies the FEM and BEM formulations. These generalized tensors are defined as follows:

$$\Sigma_{iJ} := \begin{cases} \sigma_{ij} \, , & j = J = 1,2,3 \\ D_i \, , & J = 4 \end{cases} \; , \qquad Z_{Kl} := \begin{cases} \varepsilon_{kl} \, , & k = K = 1,2,3 \\ -E_l \, , & K = 4 \end{cases} \; , \tag{6}$$

$$U_K := \begin{cases} u_k \,, & k = K = 1,2,3 \\ \varphi \,, & K = 4 \end{cases} \,, \qquad T_J := \begin{cases} t_j \,, & j = J = 1,2,3 \\ q \,, & J = 4 \end{cases} \,, \tag{7}$$

$$C_{iJKl} := \begin{cases} C_{ijkl} \,, & j = J = 1,2,3;\; k = K = 1,2,3 \\ e_{lij} \,, & j = J = 1,2,3;\; K = 4 \\ e_{ikl} \,, & J = 4; \qquad\quad k = K = 1,2,3 \\ -\epsilon_{il} \,, & J = 4; \qquad\quad K = 4 \end{cases} \,. \tag{8}$$

In this condensed notation, the motion and electric field of a piezoelectric body can now be described by

$$\mathcal{L}_{JK}\, U_K(x_i) = \mathcal{B}_{JK} U_K(x_i) \,, \qquad x_i \in \Omega \subset I\!R^3 \tag{9}$$

with boundary conditions

$$U_J = \bar{U}_J \qquad \text{on} \qquad \Gamma_U \,, \tag{10}$$

$$T_J = \bar{T}_J \qquad \text{on} \qquad \Gamma_T \,, \tag{11}$$

and initial conditions

$$U_J(t=0) = U_J^0 \,, \tag{12}$$

$$\dot{U}_J(t=0) = \dot{U}_J^0 \,. \tag{13}$$

In Eqn (9), $\mathcal{L}_{JK} := C_{iJKl}\partial_i\partial_l$ is the elliptic operator of static piezoelectricity, and $\mathcal{B}_{JK} := \rho\,\tilde{\delta}_{JK}\,\partial_t^2$ is a differential operator, which describes the effects of inertia. A modified Kronecker delta has been introduced, accounting for the fact that the electric field is assumed to be quasi-static:

$$\tilde{\delta}_{JK} := \begin{cases} \delta_{jk} \,, & j = J = 1,2,3 \,, \quad k = K = 1,2,3 \\ 0 \,, & \text{otherwise} \end{cases} \tag{14}$$

4 FEM and BEM for Piezoelectric Continua

4.1 Finite Element Method

Finite Element Methods for dynamic piezoelectricity are already well established (see e.g. Allik and Hughes (1970) and Lerch (1990)). Therefore, only a brief review is given here, using the condensed notation. The starting point of the FE formulation is the following variational principle (Allik and Hughes, 1970):

$$\int\limits_{\Omega} (\Sigma_{iJ}\,\delta Z_{Ji} + \rho\,\ddot{u}_i\,\delta u_i)\;\mathrm{d}\Omega = \int\limits_{\Gamma_T} \bar{T}_I\,\delta U_I\;\mathrm{d}\Gamma \,. \tag{15}$$

In order to apply the FEM, the piezoelectric body is subdivided into a finite number N_E of domain elements, the so-called *finite elements*, as shown in Figure 1. These elements are mapped onto reference elements by means of a series of shape functions Φ^q and nodal coordinates $\breve{x}_i^q$

$$x_i(\xi,\eta,\zeta) \approx \sum_{q=1}^{N} \Phi^q(\xi,\eta,\zeta)\;\breve{x}_i^q \,, \tag{16}$$

where N is the number of nodes of the respective element, $\check{(\cdot)}$ denotes nodal values, and ξ, η, and ζ are the local coordinates in the reference element. The integrals in Eqn (15) can now be expressed by a sum of integrals over the elements.

In most Finite Element analyses, the isoparametric concept is used, which means that the field variables are approximated by the same shape functions Φ^q as used for the mapping of the elements:

$$U_I(\xi,\eta,\zeta) \approx \sum_{q=1}^{N} \Phi^q(\xi,\eta,\zeta)\, \check{U}_I^q \,. \tag{17}$$

The field variables are now replaced by these approximations, and by assembling the contributions of all finite elements one obtains a system of ordinary differential equations in time

$$\boldsymbol{M}\ddot{\check{\boldsymbol{U}}} + \boldsymbol{K}\check{\boldsymbol{U}} = \check{\boldsymbol{Q}} \,. \tag{18}$$

The mass matrix in Eqn (18) has the form

$$\boldsymbol{M} = \begin{bmatrix} \boldsymbol{M}_{uu} & \mathbf{0} \\ \mathbf{0} & \mathbf{0} \end{bmatrix} , \tag{19}$$

reflecting the absence of electric inertia effects due to the quasi-static approximation of the electric field.

4.2 Boundary Element Methods

While the FEM for dynamic piezoelectricity is already well established, a BEM formulation has only recently been developed by the authors (Kögl and Gaul, 1999; Kögl and Gaul, 2000). This Boundary Element formulation starts with the piezoelectric reciprocity relation

$$\int_{\Omega} \left(\mathcal{L}_{JK}U_K\, U^*_{MJ} - \mathcal{L}_{JK}U^*_{MK}\, U_J\right)\, \mathrm{d}\Omega = \int_{\Gamma} \left(U^*_{MJ}\, T_J - T^*_{MJ}\, U_J\right)\, \mathrm{d}\Gamma \,, \tag{20}$$

where U^*_{MJ} and T^*_{MJ} are the generalized displacement and traction fundamental solutions of the static piezoelectric operator, defined by

$$\mathcal{L}_{JK}U^*_{MK} = -\delta_{JM}\, \delta(x_i,\xi_i) \qquad \text{and} \qquad T^*_{MJ} := C_{iJKl}\, U^*_{MK,l}\, n_i \,. \tag{21}$$

By replacing the expressions in the domain integral with Eqns (9) and (21), one obtains a piezoelectric representation formula

$$U_M(\xi) = \int_{\Gamma} \left(U^*_{MJ}\, T_J - T^*_{MJ}\, U_J\right)\, \mathrm{d}\Gamma - \int_{\Omega} U^*_{MJ}\mathcal{B}_{JK}U_K\, \mathrm{d}\Omega \,. \tag{22}$$

The remaining domain integral, which results from the use of the static fundamental solution and contains the effects of inertia, can be transformed to the boundary using the Dual Reciprocity Method. To this end, the domain term is approximated by a series of tensor functions f^q_{JN} and unknown coefficients α^q_N

$$\mathcal{B}_{JK}U_K(x) \approx \sum_{q=1}^{N} f^q_{JN}(x)\, \alpha^q_N \,, \tag{23}$$

so that, by substituting the approximation (23) into Eqn (22), a new representation formula for the generalized displacement field can be obtained

$$U_K(\xi) = \int_\Gamma (U^*_{KJ}\, T_J - T^*_{KJ}\, U_J)\, \mathrm{d}\Gamma$$
$$+ \sum_{q=1}^{N} \left(U^q_{KN}(\xi) + \int_\Gamma (T^*_{KJ}\, U^q_{JN} - U^*_{KJ}\, T^q_{JN})\, \mathrm{d}\Gamma \right) \alpha^q_N \,, \tag{24}$$

representing $U_K(\xi)$, $\xi \in \Omega$ in terms of field quantities on the boundary only. The particular solutions U^q_{JN} and T^q_{JN}, which appear in Eqn (24), are defined by

$$\mathcal{L}_{JK}\, U^q_{KN} = f^q_{JN} \qquad \text{and} \qquad T^q_{JN} := C_{iJKl}\, U^q_{KN,l}\, n_i \,. \tag{25}$$

From Eqn (24) the internal displacements $U_K(\xi)$ can be calculated at any point $\xi \in \Omega$ if the boundary variables and the coefficients α^q_N are known.

The next step is the discretization of the model into finite elements on the boundary, the so-called *boundary elements*, as shown in Figure 1. Similar to Finite Element analyses, the boundary elements are mapped onto reference elements, and the field variables U_I and T_I are approximated by a series of shape functions and nodal values

$$x_i = \sum_{q=1}^{N} \Phi^q\, \check{x}^q_i \,, \qquad U_I = \sum_{q=1}^{N} \Phi^q\, \check{U}^q_I \,, \qquad T_I = \sum_{q=1}^{N} \Phi^q\, \check{T}^q_I \,, \tag{26}$$

where N is the number of local nodes of the respective boundary element. Now, the load point ξ in the representation formula (24) is transferred to the boundary, which leads to the boundary integral equation (BIE). Finally, the approximations (26) can be introduced, so that a system of equations

$$\boldsymbol{M}\ddot{\check{\boldsymbol{U}}} + \boldsymbol{H}\check{\boldsymbol{U}} = \boldsymbol{G}\check{\boldsymbol{T}} \tag{27}$$

can be assembled by summation over the boundary elements. This system is similar to Eqn (18) obtained in Finite Element analysis, but as usual in BEM analysis the system matrices are not symmetric. In addition, the piezoelectric mass matrix obtained with the present BE formulation contains a non-diagonal entry

$$\boldsymbol{M} = \begin{bmatrix} \boldsymbol{M}_{uu} & \boldsymbol{0} \\ \boldsymbol{M}_{\varphi u} & \boldsymbol{0} \end{bmatrix} , \tag{28}$$

resulting from the fact that the particular solution fields are coupled. However, this term does not present any problems in the solution process, as shown in the following section.

5 Solution of the Systems of Equations

Comparing the systems (18) and (27) obtained with the piezoelectric FE and BE formulations, one sees that the BEM equations are of a mixed type, containing unknown generalized displacements and fluxes, while the FEM system contains only generalized displacements. By subdividing the vectors and matrices into known and unknown parts, denoted by the superscripts ‘k’ and 'u', it is possible to eliminate the unknown fluxes $\boldsymbol{T}^{\mathrm{u}}$ from the equations (27) (the symbol $\check{(\cdot)}$ denoting nodal values is omitted in the following). This leads to

$$\boldsymbol{M}^{\mathrm{u}}\ddot{\boldsymbol{U}}^{\mathrm{u}}(t) + \boldsymbol{K}^{\mathrm{u}}\boldsymbol{U}^{\mathrm{u}}(t) = \boldsymbol{Q}^{\mathrm{k}}(t) \,, \tag{29}$$

where the matrices $\boldsymbol{M}^{\mathrm{u}}$, $\boldsymbol{K}^{\mathrm{u}}$ and vector $\boldsymbol{Q}^{\mathrm{k}}$ result from the condensation (for a more detailed description of the solution process, see Kögl (2000)). Eqn (29) has now the same form as the FEM system in Eqn (18).

Next, the unknown displacement vector is split into an elastic part, denominated by the subscript 'u', and an electric part, denominated by the subscript 'φ':

$$\begin{bmatrix} \boldsymbol{M}^{\mathrm{u}}_{uu} & \boldsymbol{0} \\ \boldsymbol{M}^{\mathrm{u}}_{\varphi u} & \boldsymbol{0} \end{bmatrix} \begin{bmatrix} \ddot{\boldsymbol{u}}^{\mathrm{u}}(t) \\ \ddot{\boldsymbol{\varphi}}^{\mathrm{u}}(t) \end{bmatrix} + \begin{bmatrix} \boldsymbol{K}^{\mathrm{u}}_{uu} & \boldsymbol{K}^{\mathrm{u}}_{u\varphi} \\ \boldsymbol{K}^{\mathrm{u}}_{\varphi u} & \boldsymbol{K}^{\mathrm{u}}_{\varphi\varphi} \end{bmatrix} \begin{bmatrix} \boldsymbol{u}^{\mathrm{u}}(t) \\ \boldsymbol{\varphi}^{\mathrm{u}}(t) \end{bmatrix} = \begin{bmatrix} \boldsymbol{Q}^{\mathrm{k}}_{u}(t) \\ \boldsymbol{Q}^{\mathrm{k}}_{\varphi}(t) \end{bmatrix} . \tag{30}$$

When $\boldsymbol{M}^{\mathrm{u}}_{\varphi u} \equiv 0$, Eqn (30) applies to FEM, too.

It is now possible to eliminate the electric degrees of freedom, reducing the piezoelectric system (30) to a purely elastic one

$$\bar{\boldsymbol{M}}^{\mathrm{u}}\ddot{\boldsymbol{u}}^{\mathrm{u}}(t) + \bar{\boldsymbol{K}}^{\mathrm{u}}\boldsymbol{u}^{\mathrm{u}}(t) = \bar{\boldsymbol{Q}}^{\mathrm{k}}(t) \,, \tag{31}$$

where the condensed matrices $\bar{\boldsymbol{M}}^{\mathrm{u}}$ and $\bar{\boldsymbol{K}}^{\mathrm{u}}$ and vector $\bar{\boldsymbol{Q}}^{\mathrm{k}}$ contain the influence of the electric field on the elastic deformation. Eqn (31) can be solved with standard time-stepping algorithms such as Houbolt, Newmark, Wilson-θ, etc., yielding the unknown displacements at every time step. When the displacement field is known, the calculation of the unknown electric variables and fluxes at the current time step is straightforward.

6 Example

The piezoelectric body shown in Fig. 3 is subjected to a Heaviside type loading at the specified face. The material used in the computations is a piezoelectric ceramic, poled in x_3-direction, with transversely isotropic material properties. Its elastic and piezoelectric moduli, and relative permittivities, are given by

$$\begin{aligned}
&C_{11} = 107600\,\text{MPa}\ , C_{33} = 100400\,\text{MPa}\ , C_{12} = 63120\,\text{MPa}\ , \\
&C_{13} = 63850\,\text{MPa}\ ,\ \ C_{44} = 19620\,\text{MPa}\ , \\
&e_{31} = -9.6\,\text{N/Vm}\ ,\ \ e_{33} = 15.1\,\text{N/Vm}\ ,\ \ e_{15} = 12.0\,\text{N/Vm}\ , \\
&\epsilon^{\mathrm{rel}}_{11} = 1936\ ,\qquad \epsilon^{\mathrm{rel}}_{33} = 2109\ ,
\end{aligned} \tag{32}$$

the mass density is $\rho = 7800$ kg/m^3. Also, the following relations hold between the moduli: $C_{22} = C_{11}$, $C_{23} = C_{13}$, $C_{66} = 0.5(C_{11} - C_{12})$, $e_{32} = e_{31}$, $e_{24} = e_{15}$, $\epsilon^{\mathrm{rel}}_{22} = \epsilon^{\mathrm{rel}}_{11}$.

The transient response has been calculated using both the FEM and the BEM formulation presented in Section 4. The discretization of the body is shown in the figure. It consists of 375 finite elements and 350 boundary elements. Two FEM computations have been performed, the first using 8-node brick elements (*linear FEM*, 2304 dof), the second with 20-node brick elements (*quadratic FEM*, 8304 dof). For the BEM calculation, 4-node boundary elements have been used,

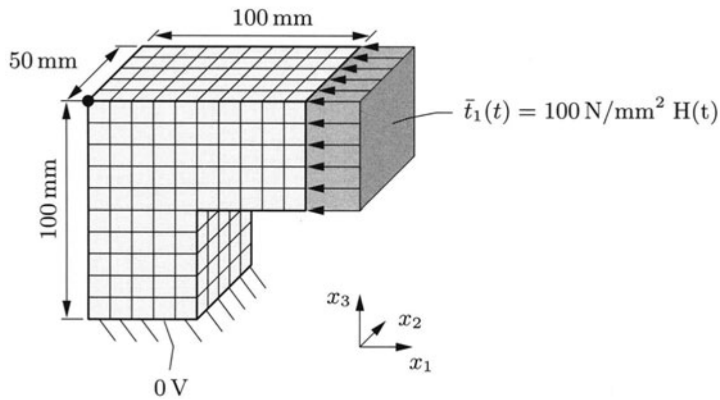

Figure 3. Piezoelectric body with discretization and boundary conditions

along with 99 internal nodes, resulting in a total of 1804 degrees of freedom. The use of internal nodes is not strictly necessary but enhances the accuracy of the results, since it improves the interpolation procedure introduced in the Dual Reciprocity formulation (see e.g. Kögl (2000)).

For the time integration, a damped Newmark algorithm is chosen, using a time step size of $\Delta t = 5\ \mu$s and parameters $\delta = 0.7$ and $\alpha = 0.5$ as proposed by Kögl and Gaul (1999). The time histories of the electric potential φ and velocity $\dot{u}_1$ at point $(0, 0, 100)$ are shown in Figure 4. Excellent agreement between the linear FEM and DR-BEM computations can be observed in both cases, with only a slight deviation from the more accurate results of the FEM computation using quadratic element shape functions.

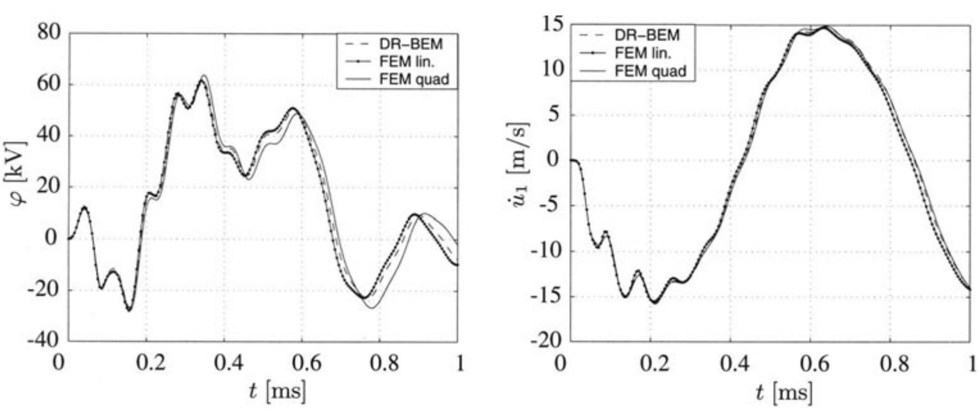

Figure 4. Electric potential $\varphi(t)$ and velocity $\dot{u}_1(t)$ at point (0,0,100)

Figure 5 shows the results obtained for the electric field E_1, and elastic stress σ_{13} at a point with the coordinates $(37.5, 12.5, 62.5)$. Taking the quadratic Finite Element calculations as reference, it can be observed that the Boundary Element computations with linear element shape functions are much more accurate than the corresponding linear Finite Element computations, for reasons which have already been explained in Section 2. This shows that the improved accuracy of the Boundary Element Methods in the calculation of flux quantities is maintained in the present piezoelectric DR-BEM.

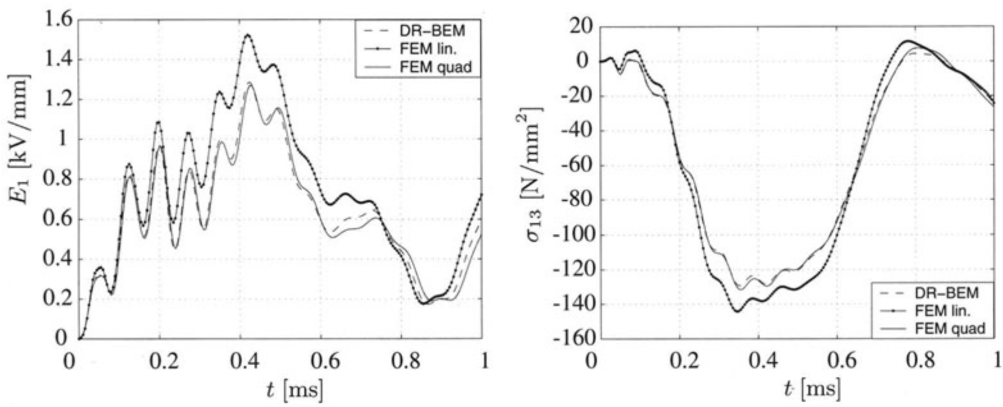

Figure 5. Electric field $E_1(t)$ and elastic stress $\sigma_{13}(t)$ at point (37.5,12.5,62.5)

7 Conclusions

A comparative study and introduction to the numerical calculation of piezoelectric continua with Finite Elements and Boundary Elements has been given. In a numerical example, excellent agreement could be demonstrated between the Finite Element results and those obtained using a Boundary Element formulation recently introduced by the authors. It could be observed that for the electric field and stress calculations, the results obtained by the new BEM formulation are more accurate than the results from Finite Element computations when using a comparable grid. This BEM formulation therefore presents a powerful numerical tool and an alternative to FEM for the computation of transient piezoelectric phenomena, especially for electric field and stress analysis.

References

Allik, H., and Hughes, T. J. R. (1970). Finite element method for piezoelectric vibration. *Int. J. Num. Meth. Eng.* 2:151–157.

Bathe, K.-J. (1996). *Finite element procedures.* New Jersey: Prentice-Hall.

Brebbia, C., Telles, J., and Wrobel, L. (1984). *Boundary element techniques.* Berlin: Springer-Verlag.

Gaul, L., and Fiedler, C. (1996). *Boundary Element Methods in Statics and Dynamics (in German).* Braunschweig: Verlag Vieweg.

Kögl, M., and Gaul, L. (1999). Dual reciprocity boundary element method for three-dimensional problems of dynamic piezoelectricity. In *Boundary Elements XXI*, 537–548. Southampton: Computational Mechanics Publications.

Kögl, M., and Gaul, L. (2000). A Boundary Element Method for transient piezoelectric analysis. *Engineering Analysis with Boundary Elements* 24(7-8):591–598.

Kögl, M. (2000). *A Boundary Element Method for Dynamic Analysis of Anisotropic Elastic, Piezoelectric, and Thermoelastic Solids*. PhD thesis, Universität Stuttgart.

Lerch, R. (1990). Simulation of piezoelectric devices by two- and three-dimensional finite elements. *IEEE Transactions on ultrasonics, ferroelectrics, and frequency control* 37(2):233–247.

Partridge, P. W., Brebbia, C. A., and Wrobel, L. C. (1992). *The dual reciprocity boundary element method.* Southampton: Computational Mechanics Publications.

Tiersten, H. F. (1969). *Linear piezoelectric plate vibrations*. New York: Plenum Press.

Zienkiewicz, O. C., and Taylor, R. L. (1991). *The finite element method*, volume 2. London: McGraw-Hill, fourth edition.

Zienkiewicz, O. C., and Taylor, R. L. (1994). *The finite element method*, volume 1. London: McGraw-Hill, fourth edition.